Magnetic characterization of the frustrated three-leg ladder compound $[(CuCl_2tachH)_3Cl]Cl_2$

Jürgen Schnack*
Universität Osnabrück, Fachbereich Physik, D-49069 Osnabrück, Germany

Hiroyuki Nojiri†
Institute for Materials Research, Tohoku University, Katahira 2-1-1, Sendai 980-8577, Japan

Paul Kögerler‡
Ames Laboratory and Department of Physics and Astronomy, Iowa State University, Ames, Iowa 50011, USA

Geoffrey J. T. Cooper and Leroy Cronin§
Department of Chemistry, The University of Glasgow, Glasgow, G12 8QQ, United Kingdom
(Received 22 March 2004; revised manuscript received 11 August 2004; published 15 November 2004)

We report the magnetic features of a one-dimensional stack of antiferromagnetically coupled equilateral copper(II) triangles. High-field magnetization measurements show that the interaction between the copper triangles is of the same order of magnitude as the intratriangle exchange although only coupled via hydrogen bonds. The infinite chain turns out to be an interesting example of a frustrated cylindrical three-leg ladder with competing intra- and inter-triangle interactions. We demonstrate that the ground state is a spin singlet which is gaped from the triplet excitation.

DOI: 10.1103/PhysRevB.70.174420 PACS number(s): 75.50.Xx, 75.10.Jm, 75.40.Cx

I. INTRODUCTION

One characteristic of magnetic molecules is that their intermolecular interaction is usually extremely weak compared to their intramolecular interactions. This becomes one of the experimental advantages when investigating these materials since a measurement at a crystal or powder of such molecules reflects the properties of a single molecule. Also for speculative applications like storage media the independence of the molecular units is crucial, for an overview see Ref. 1 and references therein.

Despite the advantages of virtually independent magnetic molecules the controlled coupling of magnetic clusters to one- or multidimensional networks is a highly interesting avenue as well, especially if the degree of magnetic exchange between the cluster entities can be varied over a wide range. Examples for such cluster-based networks are, e.g., given by chains[2] and square lattices[3,4] of the magnetic Keplerate molecule $\{Mo_{72}Fe_{30}\}$. These systems show combinations of physical properties that stem from both molecular and bulk effects.

In this paper we report the magnetic characterization of the cluster compound[5,6] $[(CuCl_2tachH)_3Cl]Cl_2$ (tach $=cis,trans$-1,3,5-triamino-cyclohexane), which contains one-dimensional arrays of antiferromagnetically coupled equilateral copper(II) ($s_{Cu}=1/2$) triangles that are aligned to form infinite stacks of antiprisms, see Fig. 1. These copper(II) triangle clusters $(CuCl_2tachH)_3Cl$ comprise a central μ_3-chloride ion that coordinates to the three copper centers in an unprecedented trigonal-planar bonding mode. In addition, this arrangement is stabilized by hydrogen bonds between the terminal chloride ligands and the NH groups from neighboring tach ligands coordinating to neighboring copper centers. As the unpaired electron of each d^9 Cu(II) center resides in a molecular orbital of dominant $d_{x^2-y^2}$ character which overlap with the ligand atoms involved in these hydrogen bonds, magnetic superexchange between the copper centers of a triangle should be restricted to this pathway, compare Fig. 2, while exchange involving the central μ_3-chloride ligand would require a significant population of the Cu d_{z^2} orbitals. Further hydrogen bonds between the $(CuCl_2tachH)_3Cl$ triangles in the crystal lattice result in an extended three-dimensional supramolecular arrangement: additional noncoordinating chloride anions interlink the triangles to *ab* planes, and an extensive network of hydrogen bonds between the terminal chloride ligands and the NH groups connect these planes together along the crystallographic *c*-axis.

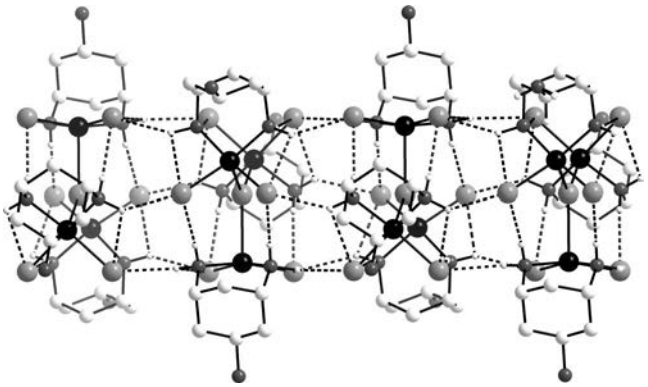

FIG. 1. The figure shows the molecular structure of the cluster framework and the dotted lines represent the hydrogen bonds which connected the triangular units to the triangular antiprismatic chain; the copper(II) ions as large black spheres, the nitrogen atoms as small black spheres, the chloride ions as large grey spheres, the carbon atoms as large white spheres, and the hydrogen atoms as small white spheres.

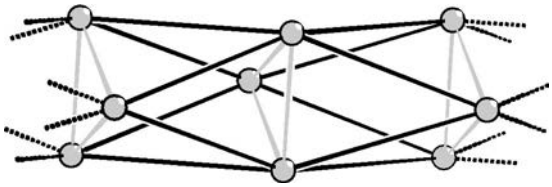

FIG. 2. Schematic structure of the triangular copper chain: The copper ions are placed at the vertices, intratriangle exchange pathways of the related Heisenberg Hamiltonian (1) are drawn by grey lines (J_1), intertriangle couplings are given by black lines (J_2).

Taking into account that the coupling between the antiferromagnetically coupled triangles is mediated by hydrogen-bonded Cu—Cl···H—N—Cu super-exchange pathways, one could conjecture that the magnetic properties of the system may be well described by weakly coupled triangles. This implies that the system at high temperatures behaves like independent triangles while at low temperatures it behaves like a linear chain of effective spins given by the ground state spin of each triangle, which is 1/2.

In a magnetization measurement such a situation would be reflected by a pronounced plateau at 1/3 of the saturation magnetization. Our high-field magnetization measurement show, however, no plateau. The observed magnetization and susceptibility curves are successfully interpreted by a theoretical model, in which the inter- and intra-triangle exchange parameters are of similar magnitude. Actually, the hydrogen-bonded super-exchange appears to be even stronger than the intratriangle exchange pathways (mediated by the bridging chloro ligand and intramolecular hydrogen bonds) although the Cu—Cu distance between triangles is 6.82 Å, whereas the intratriangle Cu—Cu distance is 4.46 Å.

From a solid state physics point of view the chain system belongs to the class of Heisenberg three-leg ladder systems with frustrated rung boundary condition, see e.g., Refs. 7–9. Such systems show a rich phase diagram and may have analytically known ground states.[7] However, the three-leg copper ladder discussed in this paper is not of the simple structure—investigated in Refs. 7–9—where one either assumes that the coupling is simpler[7] or that the rung spin is a good quantum number.[8] Nevertheless, the present structure poses an interesting frustrated three-leg ladder with two competing interactions.

The paper is organized as follows. In Sec. II we report our experimental results followed by a discussion of the theoretical model in Sec. III. The last section outlines the behavior of our three-leg ladder for fictitious intra- and inter-triangle couplings.

II. EXPERIMENTAL RESULTS

The susceptibility χ was measured for $[(CuCl_2tachH)_3Cl]Cl_2$ using a superconducting quantum interference device (SQUID) magnetometer (Quantum Design MPMS-5) at $B=0.5$ T in a temperature range of $2-290$ K. The resulting dependence is shown as a solid curve in Fig. 3. Figure 4 displays the related dependence of $T\chi$ on temperature. Here the thin dashed line marks the high temperature limit for an equivalent system of three uncorrelated $s=1/2$ centers.

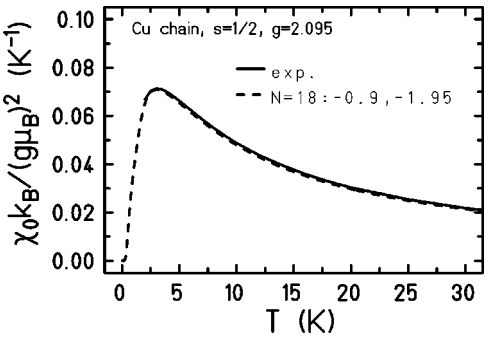

FIG. 3. Magnetic low-field susceptibility χ_0 per copper triangle: The solid curve shows the experimental result obtained at $B=0.5$ T down to temperatures of 2 K. The dashed curve displays the zero-field susceptibility of an isotropic Heisenberg model, compare Eq. (1), with exchange parameters $J_1=-0.9$ K and $J_2=-1.95$ K as given in the figure.

To establish the g values of $[(CuCl_2tachH)_3Cl]Cl_2$ electron spin resonance (ESR) measurements have been performed at 190 GHz with a powder sample by using pulsed magnetic fields and Gunn oscillators.[10] A typical powder pattern has been found. We fitted the ESR spectrum determined at 30 K, where one can neglect the effect of short range order, compare Fig. 4. The spectrum can be very well reproduced by assuming a uniaxial anisotropy of the g value with $g_\parallel=2.06\pm0.02$ and $g_\perp=2.12\pm0.02$. These g values can be interpreted by considering the local environment of Cu^{2+} ions as follows. Cu^{2+} is in pyramidical coordination and the apical bonds are in the plane normal to the chain (ab plane). The lengths of the two bonds in the basal plane of each pyramid are nearly the same and thus the g-value anisotropy in the basal plane is small. In this case, we can define the local g value along the apical bond as g_a and in the basal plane as g_b. Note that directions of the apical bonds alter by 120° between nearest neighbor Cu^{2+} ions in a triangle. Therefore, the effective g value of coupled copper ions in the ab plane is the average of g_a and g_b with some weak threefold anisotropy. The g-value anisotropy in the ab plane for the threefold symmetry of a triangle cannot be seen in the

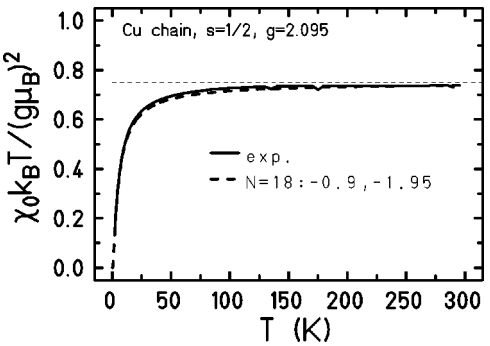

FIG. 4. Magnetic low-field susceptibility $T\chi_0$ per copper triangle: Again the solid curve shows the experimental result, the dashed curve the theoretical one. The thin horizontal line is the high temperature limit.

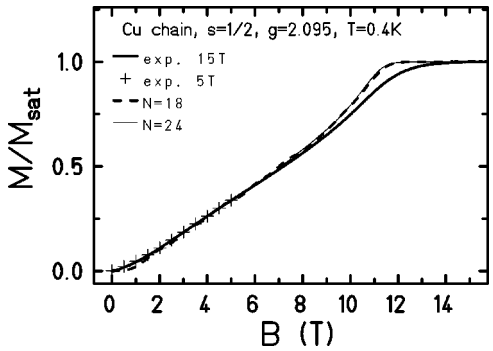

FIG. 5. Magnetization per copper triangle: Experimental data taken at a cryostat temperature of 0.4 K are given by thick solid lines, the two data sets are practically identical. The theoretical estimates using the same parameters as in Fig. 3 are given for 18 and 24 spins, i.e., 6 or 8 triangles. The saturation field is $B_{\mathrm{sat}}=11$ T.

present experiment due to the use of a powder sample. If a single crystal was used, the threefold pattern may be observed at very high frequency (>600 GHz) where the anisotropy of the Zeeman energy is much larger than the exchange coupling. Further, the effective g value along the chain corresponds to g_b, because it is common for all triangles. Accordingly, we can expect a uniaxial g-value anisotropy, where g_b is close to $g_{\parallel}$ and $g_{\perp}$ is the average of g_a and g_b. For the theoretical studies of Sec. III we are using an average g value of 2.095.

The high-field magnetization of $[(CuCl_2tachH)_3Cl]Cl_2$ has been measured in pulsed magnetic fields at the Okayama high magnetic field laboratory by using a standard inductive method (maximum $B=40$ T, $dB/dt=10\,000\ldots150\,000$ T/s). The sample is immersed in liquid ^{3}He to keep a good contact with the thermal bath. No clear hysteresis is found between up and down sweeps, see Fig. 5. In addition static-field measurements were performed up to 5 T which perfectly agree with the pulsed-field results. Thus we conclude that the measured magnetization curve shows an isothermal magnetization. Nevertheless, the experimental curve deviates from the theoretical one, see Sec. III below, especially in the vicinity of the saturation field $B_{\mathrm{sat}}=11$ T. It might very well be that the g-value anisotropy or a staggered field, which is possible in the present crystal structure, are the origin of the stronger rounding of the experimental data. The effect of a staggered field is strongly enhanced in higher fields since it grows with the external field strength, see, e.g., Ref. 11 where a linear dependence between staggered and external field is assumed which leads to rounding effects (due to mixing of states) that are quadratic in the staggered field.

The small difference between experimental and theoretical curves at low fields is due to the fact that a finite chain has a larger singlet-triplet gap compared to the infinite chain, see Fig. 8.

III. THEORETICAL MODEL

Our electron paramagnetic resonance (EPR) measurements suggest only weak anisotropy, therefore we model the system by an isotropic Heisenberg Hamiltonian

$$\underset{\sim}{H} = -\sum_{u,v} J_{uv}\vec{\underset{\sim}{s}}(u)\cdot\vec{\underset{\sim}{s}}(v) + g\mu_B\vec{B}\cdot\vec{\underset{\sim}{S}}, \tag{1}$$

where $\vec{\underset{\sim}{s}}(u)$ are the individual spin operators at sites u, $\vec{\underset{\sim}{S}}$ is the total spin, and $\underset{\sim}{S}_z$ its z-component. The homogeneous magnetic field defines the z direction. The spin quantum number of the copper ions is $s=1/2$. J_{uv} are the matrix elements of the symmetric coupling matrix. A negative value of J_{uv} corresponds to antiferromagnetic coupling.

Using the fact that the Hamiltonian, the total spin, its z component as well as the point-group symmetry operations commute with each other it is possible to diagonalize the Hamiltonian of finite chains numerically exactly. Thus all the thermodynamic quantities can be evaluated without approximation. We determined the complete spectra of two, four, and six triangles with a cyclic boundary condition in order to estimate the unknown intratriangle exchange parameter J_1 as well as its intertriangle counterpart J_2. For eight triangles the spectrum could still be determined for Hilbert subspaces with large enough magnetic quantum number M. Since the resulting magnetization does not differ from those of a six-triangle chain, see Fig. 5, we can safely assume that a chain of six triangles already reflects the properties of the infinite chain to a very large extent.

Figures 3–5 show the theoretical curves for the zero-field susceptibility as well as for the magnetization, which we obtain for $J_1=-0.9$ K and $J_2=-1.95$ K. The magnetization curve turns out to be crucial for an understanding of the exchange parameters. If the intratriangle coupling was much stronger than the intertriangle coupling, then the magnetization curve would show a pronounced plateau at $1/3$ of the saturation magnetization. This can be understood by looking at an equilateral triangle of spins $s=1/2$. In such a triangle there are only two energy levels, one for total spin $S=1/2$, the other for $S=3/2$, both levels are fourfold degenerate. At $T=0$ the magnetization is $1/2$ for low fields until one reaches the field where the lowest Zeeman level of $S=3/2$ crosses the former ground state level. Thus, in such a triangle the $T=0$ magnetization curve has a long plateau and one jump to saturation, compare also Fig. 7. For weakly coupled triangles this plateau starts to shrink from both sides until it vanishes for couplings of the same order. This situation holds for the investigated compound, compare Fig. 5, therefore, this chain is an example of a frustrated spin system with competing interactions.

Figure 6 shows the energy eigenvalues as a function of total spin for the finite chain with six triangles. The ground state is a singlet which is clearly separated from the first triplet excitation. There are no singlet intruders below the triplet state which sometimes is a sign of strong frustration.[12]

IV. ZERO-TEMPERATURE BEHAVIOR OF THE NEW THREE-LEG LADDER

The magnetism of the three-lag ladder shown in Fig. 2 exhibits three extremes depending on J_1 and J_2. If the intertriangle exchange parameter J_2 is equal to zero the chain

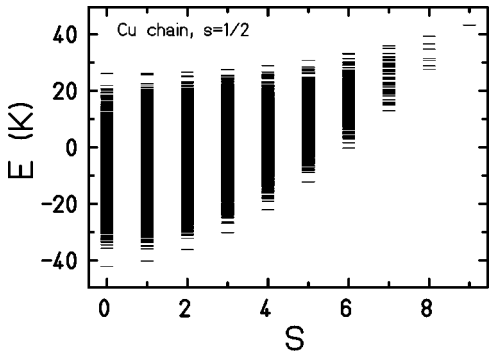

FIG. 6. Energy eigenvalues for a finite chain of six triangles using the exchange parameters given in Fig. 3.

decays into independent triangles, if the intratriangle exchange parameter J_1 is zero the three-lag ladder transforms into a square lattice wrapped around a torus, and if $J_1 = J_2 < 0$ the three-lag ladder is a triangular lattice on a torus.

From a classical point of view the ground states and the magnetization curves for $T=0$ are analytically known for all combinations of antiferromagnetic couplings J_1 and J_2.[13] Here we will discuss the special cases $J_1=0$, $J_2<0$ and $J_1<0$, $J_2=0$ as well as $J_1=J_2<0$. In the first case $J_1=0$, $J_2<0$ the system is bipartite and the classical ground state shows collinear Néel order. In the other two cases the ground state is coplanar with relative angles of 120° between neighboring spins because of three colorability of the spin system.[14,15] It can be shown that these two states always constitute a ground state. For $|J_1|<2/3|J_2|$ the collinear Néel state is ground state, for $|J_1|>2/3|J_2|$ the 120° arrangement becomes ground state.[13] For all antiferromagnetic couplings the ground state has no chiral structure. In addition the minimal energies form a parabola as a function of total spin S, therefore the magnetization curve for $T=0$ increases linearly up to saturation.

In the following we discuss the behavior of a finite quantum-spin chain of eight triangles for various combinations of J_1 and J_2. Figure 7 shows magnetization curves for $T=0$ for various hypothetical couplings. The dotted curve shows the magnetization of independent triangles ($J_2=0$), the dashed curve displays the behavior if both couplings are of

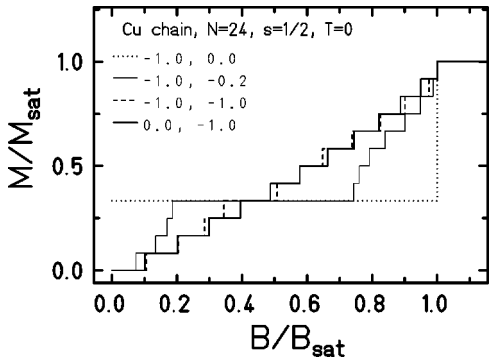

FIG. 7. Magnetization curves for $T=0$ for various hypothetical couplings of a chain of eight triangles with cyclic boundary condition. The used combinations of J_1 and J_2 are given in the figure together with the respective line mode.

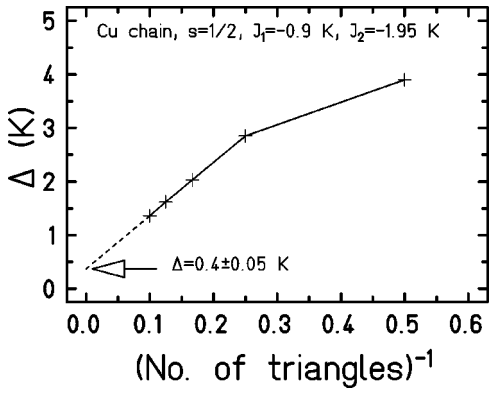

FIG. 8. Finite size extrapolation of the singlet-triplet gap for $[(CuCl_2tachH)_3Cl]Cl_2$. The gap for the infinite chain is estimated to be $\Delta \gtrapprox 0.4 \pm 0.05$ K.

equal size, and the solid curve denotes the magnetization for vanishing intratriangle coupling ($J_1=0$). The thin curve gives an example for weakly coupled triangles ($J_1=1$, $J_2=0.2$).

The discussion of independent triangles can be kept rather short, since this system can be analytically solved. For $s=1/2$ the ground state has $S=1/2$ and the first (and sole) excited state has $S=3/2$. Both are fourfold degenerate. The magnetization consists of a long plateau at $1/3$ saturation magnetization with a single jump to saturation.

The opposite case with vanishing intratriangle coupling is related to the square lattice in the sense that the triangular chain in this case is a square lattice on a torus which extends infinitely only along one direction. In the orthogonal direction the lattice has a periodic boundary condition with a period of three spins. Since the system is bipartite the theorems of Lieb, Schultz, and Mattis apply,[16,17] i. e., the ground state has $S=0$ and is nondegenerate.

The symmetric case with $J_1=J_2<0$ corresponds to a triangular lattice on a torus which extends infinitely only along one direction and again has a periodic boundary condition with a period of three spins in the orthogonal direction, see also Refs. 18 and 19. Although it is nowadays accepted that the triangular lattice has an ordered ground state and gapless magnetic excitations,[20] these properties do not automatically extend to the triangular chain due to the different dimensionality. It is very likely that the ground state is not ordered because the chain is quasi-one-dimensional.

The magnetization curves of finite systems for the cases $J_1=0$, $J_2<0$ and $J_1=J_2<0$ look rather featureless, resembling an almost regular staircase with no prominent plateau or jump. The cases interpolating between uncoupled and coupled triangles show a plateau at $1/3$ saturation magnetization, which is longer or shorter depending on the ratio of inter- and intra-triangle coupling.

After having discussed the properties of finite chains it is of course desirable to deduce properties of the infinite chain under investigation. For $[(CuCl_2tachH)_3Cl]Cl_2$ the ground state and the singlet-triplet gap can be evaluated using a Lanczos procedure for systems up to ten triangles. All finite size calculations result in a ground state spin $S=0$ which is separated by a finite gap from the triplet state, compare Fig. 6. Using chains with up to ten triangles enables us to ex-

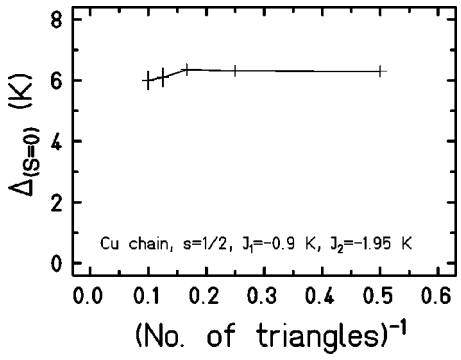

FIG. 9. Finite size behavior of the singlet-singlet gap for $[(CuCl_2tachH)_3Cl]Cl_2$. The two leftmost data points for eight and ten triangles have an uncertainty of about ±0.2 K due to the restricted accuracy of the Lanczos procedure for excited states.

trapolate to the infinite system, which turns out to have a ground state spin $S=0$ and a nonzero gap of $\Delta \gtrapprox 0.4 \pm 0.05$ K, compare Fig. 8. The value of the gap is very likely somewhat bigger since one can expect that the convergence changes from linear in $1/N$ to exponential[21,22] or a power law[23] like $1/N^2$ once the system size is bigger than the correlation length ξ.

The ground state of the $[(CuCl_2tachH)_3Cl]Cl_2$ chain is nondegenerate for all simulated system sizes. This behavior differs from the behavior of chains of weakly coupled triangles where a dimerization together with a twofold degeneracy of the ground state is observed.[24] With very high confidence we can also state that the big singlet-singlet gap—compare Fig. 6—does not collapse to a degenerate ground state with increasing system size, see Fig. 9. The gap is practically independent of N. The two values for eight and ten triangles have an uncertainty of about ±0.2 K due to the insufficient accuracy of the Lanczos procedure for such high-lying levels. We thus regard the slight decrease for these values as not significant.

ACKNOWLEDGMENTS

The authors thank Peter Hage for letting us utilize his Lanczos program, and we thank Andreas Honecker, Johannes Richter, Heinz-Jürgen Schmidt, as well as Jörg Schulenburg for fruitful discussions and again Heinz-Jürgen Schmidt for carefully reading the manuscript. H.N. acknowledges the support by a Grant-in-Aid for Scientific Research on Priority Areas (No. 13130204) from MEXT, Japan and by Shimazu Science Foundation. The Ames Laboratory is operated for the United States Department of Energy by Iowa State University under Contract No. W-7405-Eng-82.

*Electronic address: jschnack@uos.de
†Electronic address: nojiri@imr.tohoku.ac.jp
‡Electronic address: kogerler@ameslab.gov
§Electronic address: L.Cronin@chem.gla.ac.uk

[1] D. Gatteschi and R. Sessoli, Angew. Chem., Int. Ed. **42**, 268 (2003).
[2] A. Müller, S. K. Das, M. O. Talismanova, H. Bögge, P. Kögerler, M. Schmidtmann, S. S. Talismanov, M. Luban, and E. Krickemeyer, Angew. Chem., Int. Ed. **41**, 579 (2000).
[3] A. Müller, E. Krickemeyer, S. K. Das, P. Kögerler, S. Sarkar, H. Bögge, M. Schmidtmann, and S. Sarkar, Angew. Chem., Int. Ed. **39**, 1612 (2000).
[4] A. Müller, S. K. Das, E. Krickemeyer, P. Kögerler, H. Bögge, and M. Schmidtmann, Solid State Sci. **2**, 847 (2000).
[5] G. Seeber, P. Kögerler, B. M. Kariuki, and L. Cronin, Chem. Commun. (Cambridge) **2004**, 1580 (2004).
[6] Crystallographic data: $C_{18}H_{48}N_9Cl_9Cu_3$, $M=900.32$ g/mol, trigonal, space group $P6_3/m$ (176), $a=12.6800(20)$, $b=12.6800(20)$, $c=12.6287(13)$ Å, $V=1758.44(4)$ Å^3, $Z=2$, μ(Mo-K$_\alpha$) $=2.508$ mm^{-1}, 14 125 reflections measured, 1679 unique which were used in all calculations; structure solution and refinement as done using WINGX. Final R1=0.051 and wR2=0.126 (all data). CCDC reference numbers 221 962 and 219 624. See http://www.rsc.org/suppdata/cc/b4/b402487g/ for crystallographic data in CIF or other electronic format.
[7] K. Kawano and M. Takahashi, J. Phys. Soc. Jpn. **66**, 4001 (1997).
[8] A. Honecker, F. Mila, and M. Troyer, Eur. Phys. J. B **15**, 227 (2000).
[9] J. L. Gavilano, D. Rau, S. Mushkolaj, H. R. Ott, P. Millet, and F. Mila, Phys. Rev. Lett. **90**, 167202 (2003).
[10] H. Nojiri, M. Motokawa, K. Okuda, H. Kageyama, Y. Ueda, and H. Tanaka, J. Phys. Soc. Jpn. **72**, 109 (2003).
[11] T. Sakai and H. Shiba, J. Phys. Soc. Jpn. **63**, 867 (1994).
[12] C. Waldtmann, H. U. Everts, B. Bernu, C. Lhuillier, P. Sindzingre, P. Lecheminant, and L. Pierre, Eur. Phys. J. B **2**, 501 (1998).
[13] H.-J. Schmidt (private communication).
[14] M. Axenovich and M. Luban, Phys. Rev. B **63**, 100407 (2001).
[15] H.-J. Schmidt and M. Luban, J. Phys. A **36**, 6351 (2003).
[16] E. H. Lieb, T. Schultz, and D. C. Mattis, Ann. Phys. (N.Y.) **16**, 407 (1961).
[17] E. H. Lieb and D. C. Mattis, J. Math. Phys. **3**, 749 (1962).
[18] A. Honecker, J. Phys.: Condens. Matter **11**, 4697 (1999).
[19] S. Yoshikawa, K. Okunishi, M. Senda, and S. Miyashita, J. Phys. Soc. Jpn. **73**, 1798 (2004).
[20] L. Capriotti, Int. J. Mod. Phys. B **15**, 1799 (2001).
[21] G. von Gehlen and A. Honecker, J. Phys. A **26**, 1275 (1993).
[22] O. Golinelli, T. Jolicoeur, and R. Lacaze, Phys. Rev. B **50**, 3037 (1994).
[23] D. C. Cabra, A. Honecker, and P. Pujol, Phys. Rev. B **58**, 6241 (1998).
[24] A. Lüscher, R. M. Noack, G. Misguich, V. N. Kotov, and F. Mila, Phys. Rev. B **70**, 060405(R) (2004).